Electronic Supplementary Material (ESI) for RSC Advances.

Supplementary Information

Zigzag Gas Phases on Holey Adsorbed Layers

Hideaki Teshima[1,2], Naoto Nakamura[1], Qin-Yi Li[1,3], Yasuyuki Takata[3,4], Koji Takahashi[1,3,*]

[1] Department of Aeronautics and Astronautics, Kyushu University, Nishi-Ku, Motooka 744, Fukuoka 819-0395, Japan

[2] Department of Mechanical Engineering, Osaka University, 2-1 Yamadaoka, Suita 565-0871, Japan

[3] International Institute for Carbon-Neutral Energy Research (WPI-I2CNER), Kyushu University, Nishi-Ku, Motooka 744, Fukuoka 819-0395, Japan

[4] Department of Mechanical Engineering, Kyushu University, Nishi-Ku, Motooka 744, Fukuoka 819-0395, Japan

[*] Author to whom correspondence should be addressed: takahashi@aero.kyushu-u.ac.jp

Supplementary note 1

Figure S1 shows the interfaces between highly-ordered pyrolytic graphite (HOPG) and pure water imaged in amplitude modulation (AM) and frequency modulation (FM) modes. In Figure S1(a), which was obtained in AM mode, there are many micropancakes with smooth three-phase contact lines, which is consistent with previous reports[1,2]. By contrast, in Figure S1(b), which was obtained using FM mode, thin disordered layers can be seen, although the shapes of the overlying micropancakes are deformed. Because a small oscillation amplitude of the AFM probe increases the imaging sensitivity and decreases the load force[3], we measured the same area as in Figure S1(b) with a smaller amplitude of approximately 0.8 nm (Figure S1(c)). However, although the underlying disordered layers could be clearly observed under these parameters, the micropancakes became invisible, which was unexpected. This may be because the probe oscillating at small amplitudes constantly interacted with the gas micropancakes, thus dragging them horizontally. In contrast to the mobile nature of the micropancakes, the disordered layers are immobile[3,4] and thus could be measured even at small oscillation amplitudes, as shown in Figure S1(c). In AM mode with oscillation amplitudes larger than 10 nm, the probe intermittently taps the gas phases and thus measures them without dragging. Thus, FM-AFM is suitable for observing thin and immobile disordered layers but not mobile gas domains, whereas AM-AFM cannot measure atomically thin gases[3] but can accurately measure the shape of the mobile gas phases.

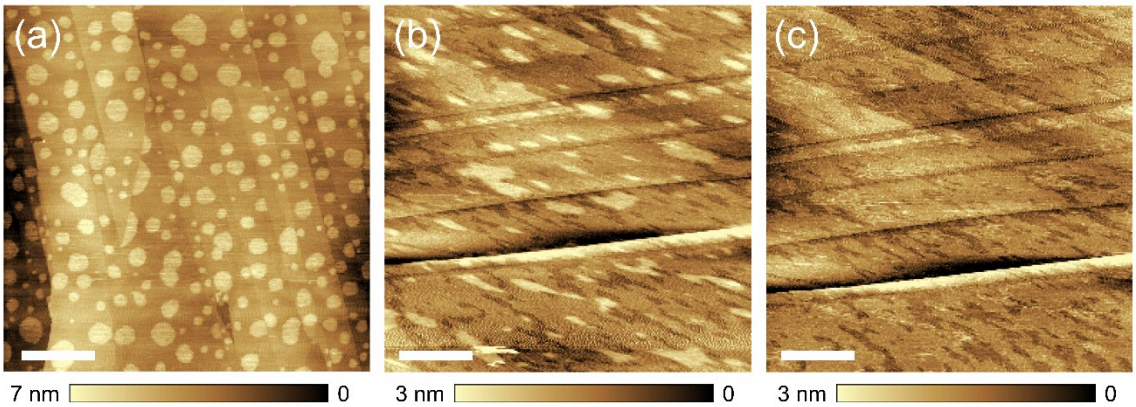

Supplementary Figure 1 Height images (5 μm × 5 μm) of an interface between highly-ordered pyrolytic graphite (HOPG) and pure water obtained in (a) AM mode, and FM mode with oscillation amplitudes of approximately (b) 3 nm and (c) 0.8 nm. The scale bars are 1 μm.

Supplementary note 2

The AFM configuration in our experiments is shown in Figure S2. By adjusting the direction of the mirrors, a red laser emitted from a laser diode reflects on the backside of an AFM probe and then is set at the center of the detector, which detects the displacement of the feedback parameters (i.e. the shift amount of the oscillation amplitude or the resonance frequency). We used a special probe holder for the measurements in liquids, which was purchased from Shimadzu Corp. The liquid cell with a depth of ~5 mm was also purchased from Shimadzu Corp. The liquid temperature was measured using a micro-thermometer, which was inserted through a hole in the probe holder. The HOPG substrate was glued to the bottom of the glass liquid cell with epoxy glue (EPOTEK 377, Epoxy Technology, Inc.). This two-component glue is strongly resistant to many solvents, including alcohols.

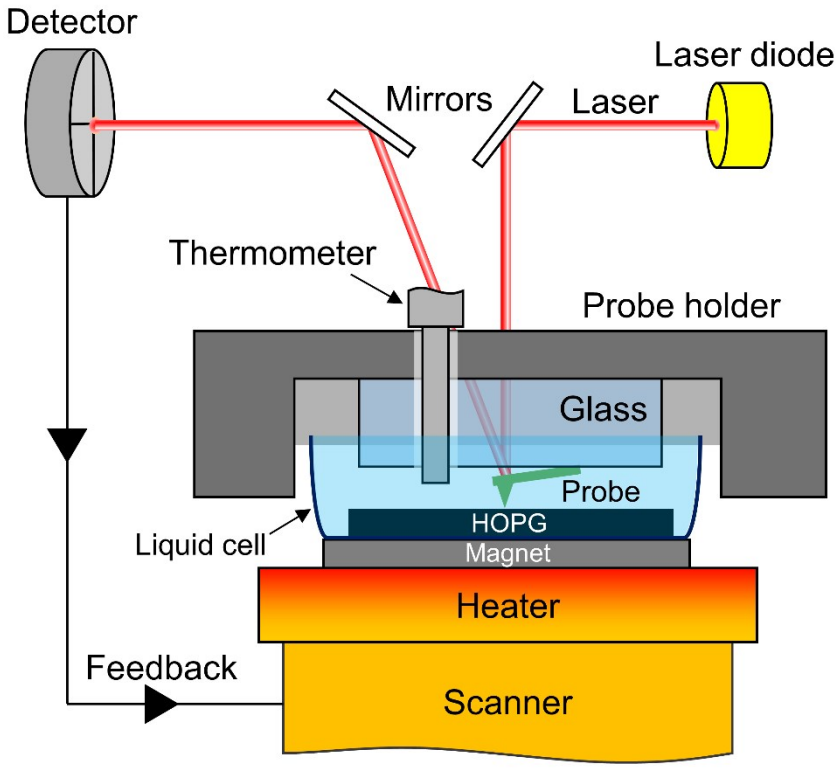

Supplementary Figure 2 Schematic image of the setup for AFM measurements in liquid.

Supplementary note 3

Figure S3(a) shows the HOPG/pure water interface before heating. Many nanobubbles were observed on the entire HOPG surface. After heating (Figure S3(b)), the nanobubbles exhibited two types of behavior: some remained, whereas others disappeared. This may be because heating promoted Ostwald ripening, in which gas molecules are transported from small nanobubbles to large nanobubbles through the liquid phase.

Figure S3(c) shows that the contact angles from the gas side of the nanobubbles became larger after heating. Assuming that the nanobubbles are in an equilibrium state, the equilibrium contact angles are described as follows[5]:

$$\sin\theta_e = \zeta\frac{L}{L_c} \tag{S1}$$

where ζ is the gas oversaturation; L is the footprint diameter; and L_c is a constant, which is defined as $L_c = \frac{4\gamma_{LV}}{P_0} = 2.84\ \mu m$, where γ_{LV} is the liquid/vapor surface tension and P_0 is the atmospheric pressure. By applying Eq. (S1) to Figure S3(c), the gas oversaturation, ζ, near the solid/liquid interface before and after heating was estimated. Accordingly, this increased from $0 < \zeta < 0.6$ before heating to $0.6 < \zeta < 1.7$ after heating. This result clearly shows that the heating procedure

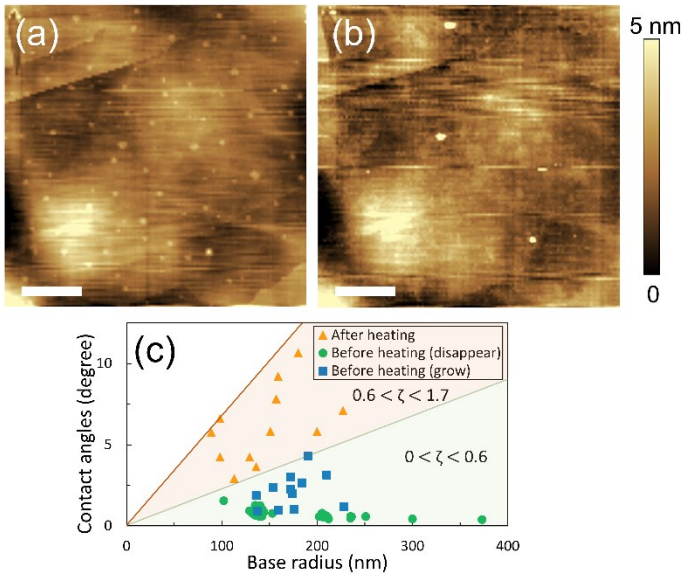

increases the gas oversaturation at the HOPG/water interface.

Supplementary Figure 3 Height images (10 μm × 10 μm) of nanobubbles at an HOPG/pure water interface (a) before and (b) after heating. The scale bars are 2 μm. (c) Scatter plot of the contact angles from the gas side of the surface nanobubbles as a function of the base radius. The green circular and blue square symbols indicate the nanobubbles that disappeared and grew by

heating, respectively. The yellow triangles indicate the nanobubbles that remained after heating.

Supplementary note 4

We used the FM mode of an SPM-8100FM AFM (Shimadzu Corp., Japan). This mode uses the magnitude of the frequency shift as a feedback parameter, which enables us to observe the HOPG/pure water interface with higher spatial resolution than normal AM mode. However, we did not use FM mode in the main manuscript because it is strongly affected by thermal drift after heating and drags the micropancakes horizontally, and thus cannot be used to measure the precise shapes of mobile micropancakes, as mentioned in Supplementary note 1. We used a PPP-NCHR cantilever (Nanosensors; tip radius: ~10 nm; spring constant: 42 N m^{-1}), which was hydrophilized by oxygen plasma treatment immediately prior to measurement. The oscillation amplitude was 0.8 nm, which is sufficiently small to observe atomically-thin ordered layers[3].

In Figure S4(a), row-like structures were observed around the featureless disordered layers. Because the row-like structures are ~0.3 nm lower than the disordered layers, we conclude that they are ordered layers that epitaxially grow owing to the crystalline structures of the underlying graphite[3,4]. Even in the enlarged area shown in Figure S4(b), the ordered layers entirely cover the HOPG surface. Because the ordered layers can be nucleated even in degassed water[4], we conclude that they cover almost all of the HOPG surface in air-supersaturated water.

In the results presented in main manuscript, we did not observe ordered layers. This is because they cannot be measured in AM mode owing to its low sensitivity and high load force, which is consistent with previous reports[3,4].

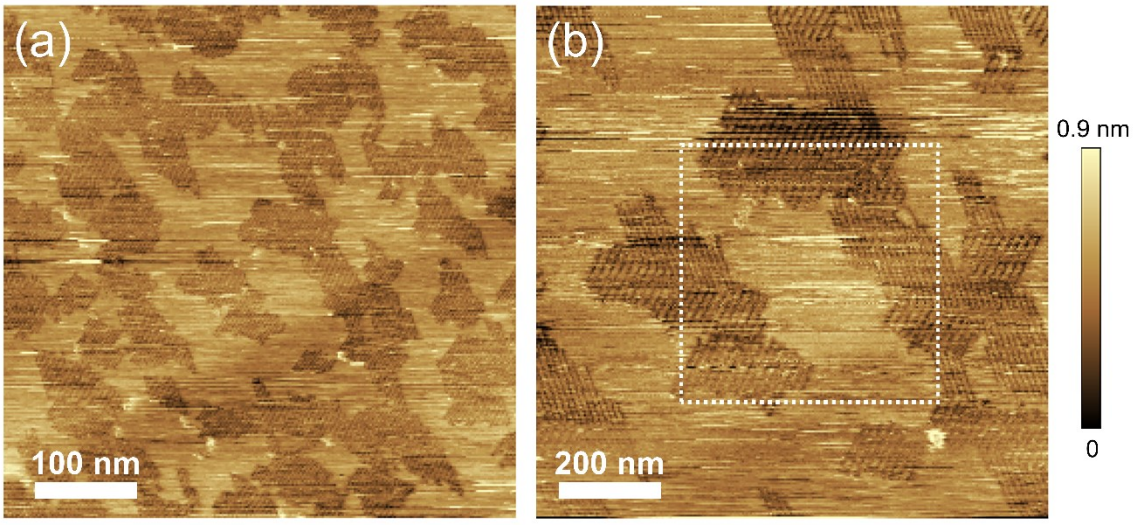

Supplementary Figure 4. High-resolution height images of disordered and ordered layers at an HOPG/pure water interface. (a) Higher-magnification (500 nm × 500 nm) image of the area marked by the white dotted line in (b) (1 μm × 1 μm).

Supplementary note 5

Figure S5(a, b) shows the broad area of the HOPG/pure water interface before and after heating. In Figure S5(a), many micropancakes and disordered layers existed widely on the HOPG surface. After heating (Figure S5(b)), a lot of holes were created in the disordered layers, while the number of them in the micropancakes was extremely smaller. Furthermore, the surface of the micropancakes was kept flat. These results are the same as those observed in the Figure 1 and 3 in the main manuscript. Note that the increase in the coverage area of the disordered layer upon heating may be caused by the direct adsorption of the dissolved gas molecules onto the HOPG surface, not by the surface-diffusion.

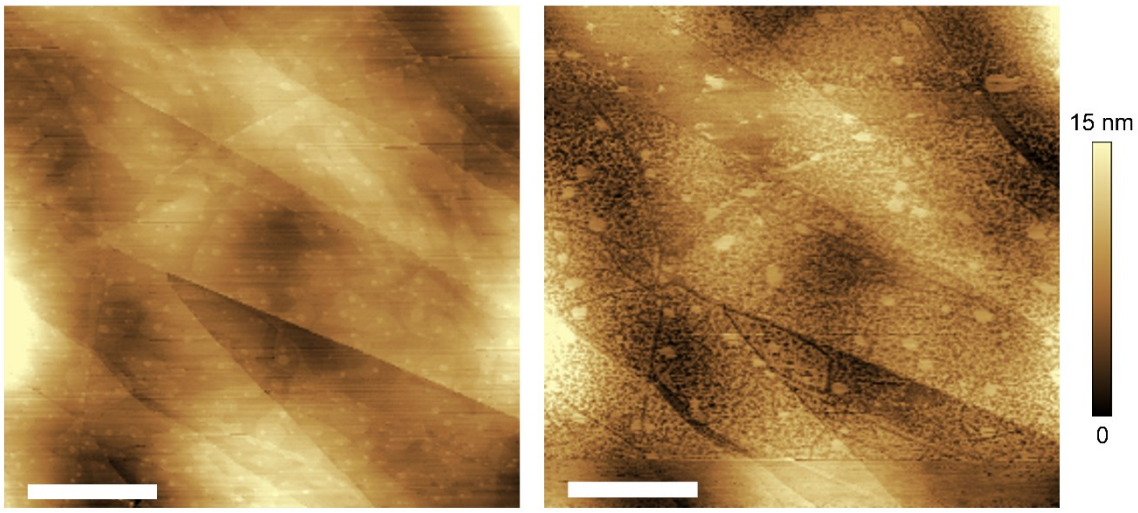

Supplementary Figure 5. Height images (20 μm × 20 μm) of micropancakes and disordered layers at an HOPG/pure water interface (a) before and (b) after heating. The scale bars are 5 μm.

Supplementary note 6

Raman spectra were measured by a commercial Raman spectrometer (LabRAM HR-800, Horiba Ltd., Japan). Figure 6 shows the Raman spectra of HOPG surfaces (a) in air, (b) in degassed water, and (c) in water after the solvent-exchange process. Although we could observe pronounced G peak at 1579 cm^{-1} and G' peak at around 2737 cm^{-1} that are characteristic peaks of graphitic materials[6] and an intensity change from 2900 to 3700 cm^{-1} relating to the OH-stretching modes of liquid water[7], no peaks originating from the micropancakes and adsorbed layers were detected. This is because these air domains are too sparse and thin (less than several nm) to be detected by the Raman spectroscopy. Thus, it is inherently difficult to obtain the Raman spectra from the adsorbed gas molecules.

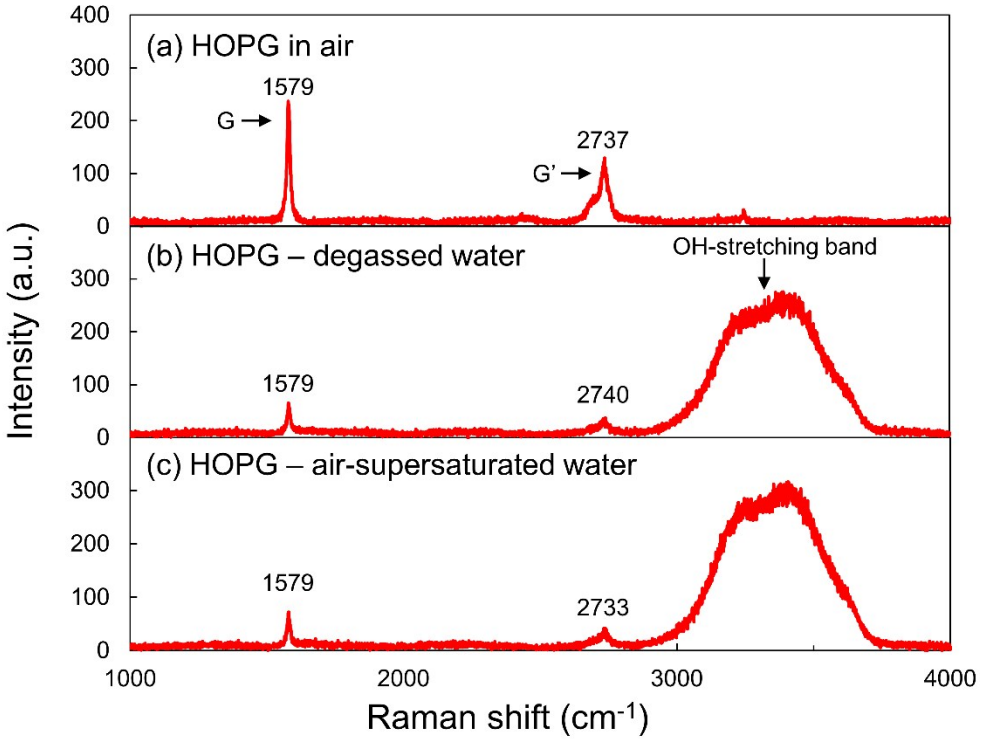

Figure S6 Raman spectra obtained at (a) HOPG in air, (b) HOPG/degassed water interface, and (c) HOPG/air-supersaturated water.

Supplementary note 7

We investigated the HOPG surface in air and in degassed water. The degassed water was prepared by boiling 400 mL of the purified water for 30 minutes. AM-AFM images obtained at HOPG surface (a, b) in air and (c, d) in degassed water are shown in Figure S7. In Figure S7(a, b), we could not observe any domains on the HOPG surface, which indicates that the HOPG surface was pristine and thus was not contaminated before injection of liquids. Similarly, the HOPG surface was not covered with anything under the degassed water as shown in Figure S7(c, d). In contrast, as shown in Figure 1 and 3 in the main manuscript and in Figure S1, S4, and S5 in the supplementary information, the broad coverage of the interfacial domains on HOPG surfaces has been repeatedly observed after the solvent-exchange process. These clearly show that the domains are formed only when the HOPG surface is immersed in air-supersaturated water.

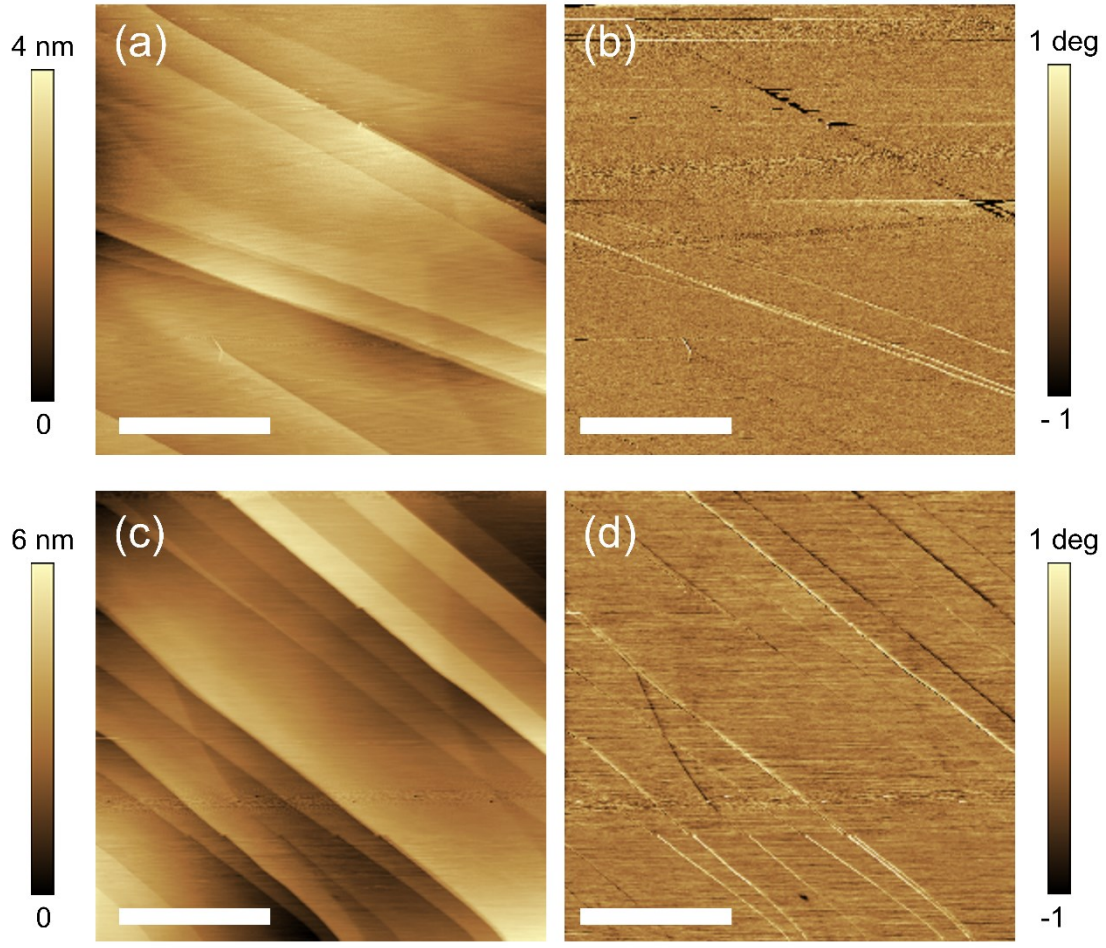

Supplementary Figure 7. Height images (3 μm × 3 μm) of HOPG surfaces (a) in air and (b) in degassed water. (b, d) Phase images corresponding to (a) and (c), respectively. The scale bars are 1 μm.

Supplementary References

1 X. H. Zhang, N. Maeda and J. Hu, *J. Phys. Chem. B*, 2008, **112**, 13671–13675.

2 X. H. Zhang, X. Zhang, J. Sun, Z. Zhang, G. Li, H. Fang, X. Xiao, X. Zeng and J. Hu, *Langmuir*, 2007, **23**, 1778–1783.

3 H. Teshima, Y. Takata and K. Takahashi, *Appl. Phys. Lett.*, 2019, **115**, 071603.

4 Y.-H. Lu, C.-W. Yang and I.-S. Hwang, *Langmuir*, 2012, **28**, 12691–12695.

5 D. Lohse and X. Zhang, *Phys. Rev. E*, 2015, **91**, 031003.

6 H. An, B. H. Tan, J. G. S. Moo, S. Liu, M. Pumera and C. D. Ohl, *Nano Lett.*, 2017, **17**, 2833–2838.

7 D. M. Carey, *J. Chem. Phys.*, 1998, **108**, 2669–2675.